Chalmers Publication Library

Effective Electron Microrefrigeration by SIN Tunnel Junctions with Advanced Geometry of Electrodes and Normal Metal Traps

(article starts on next page)

Effective electron microrefrigeration by superconductor–insulator–normal metal tunnel junctions with advanced geometry of electrodes and normal metal traps

Ian Jasper Agulo[1]**, Leonid Kuzmin**[1]**, Michael Fominsky**[1,2] **and Michael Tarasov**[1,2]

[1] Department of Microtechnology and Nanoscience, Quantum Device Physics Laboratory, Chalmers University of Technology, SE-41296 Göteborg, Sweden
[2] Institute of Radio Engineering and Electronics, 103907 Moscow, Russia

E-mail: ian.agulo@mc2.chalmers.se

Abstract
We demonstrate effective electron cooling of the normal metal strip by superconductor–insulator–normal metal (SIN) tunnel junctions. The improvement was achieved by two methods: first, by using an advanced geometry of the superconducting electrodes for more effective removal of the quasiparticles; and second, by adding a normal metal trap just near the cooling junctions. With simple cross geometry and without normal metal traps, the decrease in electron temperature is 56 mK. With the advanced geometry of the superconducting electrodes, the decrease in electron temperature is 129 mK. With the addition of the normal metal traps, the decrease in electron temperature is 197 mK.

(Some figures in this article are in colour only in the electronic version)

In the last decade superconducting detectors have become the most sensitive radiation detectors of sub-mm, infrared and optical radiation with an estimated ultimate sensitivity down to 10^{-20} W Hz$^{-1/2}$ [1]. Ultralow noise bolometers are required for space-based astronomical observations. The proposed NASA missions, SPIRE, SPIRIT and SPECS, will determine the highest level of requirements for bolometers in the near future. The detector goal is to provide a noise equivalent power less than 10^{-20} W Hz$^{-1/2}$ [2] over the 40–500 μm wavelength range in a 100×100 pixel detector array. No one existing technology could satisfy these requirements. The proposed concept of a cold-electron bolometer (CEB) with direct electron cooling [3, 4] could be a good candidate for realizing a limit performance of the detectors. The concept is based on the effect of nonequilibrium electron cooling by SIN tunnel junctions [5, 6]. In contrast to cooling of the phonon temperature on the membrane with the detector on it [7], we propose a CEB with very effective *direct electron cooling* of the absorber [3, 4]. The CEB gives the opportunity to remove incoming background power from the supersensitive region of the absorber to return the system to the lowest temperature state (T_e) to achieve the fundamental limit NEP [8]:

$$\text{NEP}^2 = 2P_0 k T_e. \quad (1)$$

For $P_0 = 10$ fW and $T_e = 50$ mK we would get the limit NEP $= 1 \times 10^{-19}$ W Hz$^{-1/2}$. The first step in this development is the realization of strong electron cooling. This work has been devoted to optimization of superconducting electrodes and normal metal traps for effective electron cooling.

The operation of a SINIS structure can be analysed using the heat balance equation [9, 10]:

$$P_{\text{cool}}(V, T_e, T_{\text{ph}}) + \Sigma \Lambda (T_e^5 - T_{\text{ph}}^5) = P_0 + \frac{V^2}{R_1} + \beta \frac{I}{e} \Delta. \quad (2)$$

Here, the cooling power
$$P_{\text{cool}}(V, T_e, T_{\text{ph}})$$
$$= \frac{1}{e^2 R} \int \mathrm{d}E \, N_S(E)(E - eV)[f_N(E - eV) - f_S(E)], \quad (3)$$
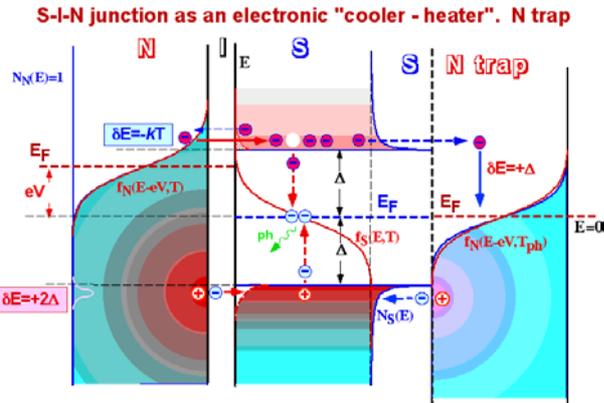
Figure 1. The energy diagram illustrating the principle of electron cooling and the problem of reabsorption of the phonons after recombination of the quasiparticles. When a bias $V \leqslant \Delta/e$ is applied across the SIN tunnel junction, only electrons with energies greater than the Fermi energy tunnel through the barrier. These electrons appear as quasiparticles in the superconductor. A quasiparticle may recombine with another quasiparticle to form a Cooper pair, and emit a phonon with energy equal to 2Δ. The emitted phonons may either be lost in the substrate or reabsorbed in the normal metal giving additional heat load to the absorber, which reduces the cooling power. Apart from quasiparticle recombination, quasiparticles near the junction also have a finite probability of tunnelling back to the normal metal.

where $\Sigma\Lambda(T_e^5 - T_{ph}^5)$ is the heat flow from electrons to the phonon subsystems in the normal metal, Σ is a material constant, Λ is the volume of the absorber, T_e and T_{ph} are, respectively, the electron and phonon temperatures of the absorber; $P_{cool}(V, T_e, T_{ph})$ is the cooling power of the SIN tunnel junctions; P_0 is the background power load, V^2/R_l is the power dissipation in the leakage resistance of the junction R_l [11] and the last term accounts for power flow due to back-tunnelling of quasiparticles and reabsorption of phonons emitted by quasiparticle recombination [12]. In simulations we have used the fifth and sixth powers of the heat flow from the phonons. The energy diagram (figure 1) illustrates the principle of the electron cooling and the problem of reabsorption of the phonons emitted by quasiparticle recombination.

The process of electron cooling is described schematically in figure 1. The SIN tunnel junction acts to cool the electrons by removing high energy thermal excitations from the normal metal to the superconductor at a bias voltage lower than the superconducting gap voltage. A normal metal trap is placed in contact with the superconductor allowing quasiparticles to be trapped and removed from the tunnel junction region. The removal of quasiparticles, further, makes the cooling of the electrons in the normal metal more effective, significantly decreasing the probability of back-tunnelling and phonon reabsorption. Therefore, in order to achieve electron cooling in the normal metal absorber, back-tunnelling and recombination processes should be prevented. In this work, we show how the advanced geometry of the superconducting electrodes and the addition of normal metal traps are effective in removing quasiparticles in the superconductor, thus enhancing the cooling of the absorber.

The first step was the fabrication of the normal metal traps. Au was chosen as the material for the traps, fabricated in the
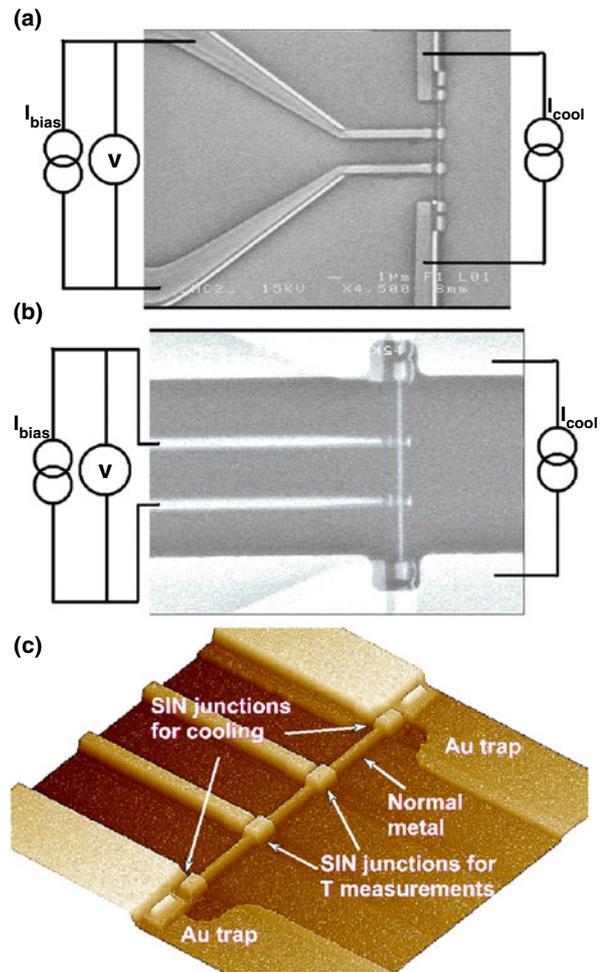

Figure 2. An SEM picture of both advanced geometry (a) and normal metal traps (b) and a typical AFM image of the structure with normal metal traps (c). The Au trap was evaporated prior to the evaporation of the Al–AlO$_x$–Cr/Cu junctions. The distance of the trap from the tunnel junction is $\approx$0.5 μm. Current bias is applied through the cooling junctions (outer junctions). The temperature of the absorber is measured from the response of the voltage across the thermometer junctions (inner junctions) with temperature with a bias current of 10 and 120 pA for the structure with and without traps, respectively. The difference in bias current values is due to the difference in area of the thermometer junctions for the structures.

same vacuum cycle as the contact pads. The patterns for the traps and the pads were formed using photolithography. Au was thermally evaporated up to a thickness of 600 Å. The next step was the fabrication of the tunnel junctions and the absorber. The structures were patterned by e-beam lithography. The metals were thermally evaporated using the shadow evaporation technique. The Al (superconductor) was evaporated at an angle of about 60° up to a thickness of 650 Å, and oxidized at a pressure of 10^{-1} mbar for 2 min. A Cr/Cu (1:1) absorber of total thickness 750 Å was then evaporated directly perpendicular to the substrate.

Figure 2 shows the two configurations of the electrodes, one with advanced geometry (a) of the two outer junctions and another with normal metal traps ((b), (c)) in addition to the advanced geometry of the two outer junctions. In the advanced geometry, the structure of the outer junctions is such that the ends of the normal metal absorber overlap with a corner of each
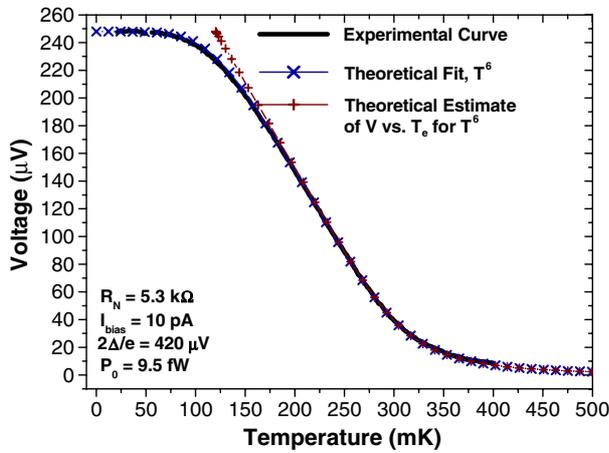
Figure 3. Calibration of the thermometer junctions: the voltage depending on the phonon temperature. The theoretical fit and the electron temperature are shown for the main calibration curve chosen for the cooling experiment with the bias current of 10 pA.

Figure 4. The main cooling curves: the electron temperature of the absorber as a function of the voltage across the cooling SIN tunnel junctions for (a) advanced geometry of the superconducting electrodes and effective Au traps ($T_{ph} = 290$ mK), (b) advanced geometry of the superconducting electrodes without traps ($T_{ph} = 295$ mK), and (c) ordinary cross geometry ($T_{ph} = 315$ mK).

of the Al electrodes, which has a much larger area compared to those for the middle Al electrodes. The inner junctions have a simple cross geometry, where a section of the normal metal absorber overlaps the thin Al electrodes. The purpose of the larger area Al electrode is to give more space for quasiparticle diffusion compared to that with the middle Al electrode with simple cross geometry. The two outer junctions have a total normal state resistance, R_N, of 2.3 kΩ, while the two inner junctions have R_N equal to 2.6 kΩ. The area of overlap, which is equivalently the area of each of the inner tunnel junctions, is equal to 0.56×0.87 μm^2. The area of each of the outer tunnel junctions is 0.55×0.82 μm^2. In the structure with normal metal traps, the area of the two outer junctions was approximately the same as that of the two outer junctions in the advanced electrode, while the area of the inner junctions was 0.2×0.3 μm^2. The outer and inner junctions have R_N equal to 0.86 and 5.3 kΩ, respectively. The volume of the absorber is 0.18 μm^3, and its resistance is 120 Ω.

A bias cooling current was applied through the outer junctions and the absorber. These junctions act as the cooling junctions, and therefore serve to decrease the electron temperature of the absorber. To determine the electron temperature, the voltage across the inner junctions was measured. This voltage is then calibrated as a function of phonon temperature. A small current bias is also applied to these junctions. The bias has to be optimal to obtain the maximum linear voltage response to temperature, and yet not so large as to disturb the cooling process in the absorber. The optimal bias current used was 10 pA. Figure 3 shows the theoretical fit and the theoretical computation of the electron temperature for the calibration curve with this bias current used for the structure with normal metal traps. The fit and computation were obtained using equations (2), (3) with power load 9.5 fW and leakage resistance 17 MΩ per junction. At around 100 mK, the curve starts to saturate. This may be due to leakage resistance and external power loading.

Figure 4 shows the main results with the electron cooling for various combinations of geometries of superconducting electrodes and effective Au traps (a)–(c). The experimental calibration curve of the measured voltage against temperature
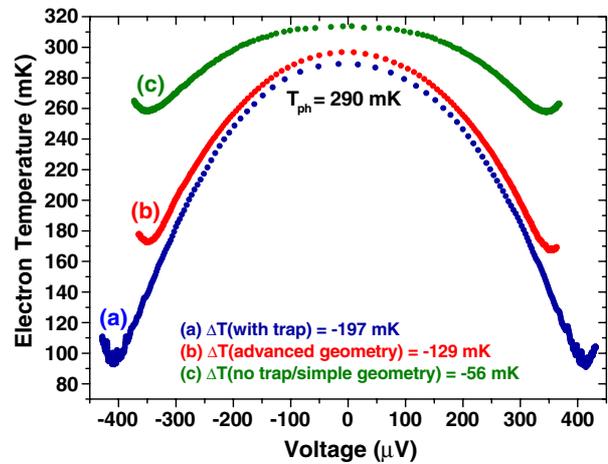
from figure 3 was used for conversion of the thermometer voltage to the temperature. A strong influence of the advanced geometry of the superconducting electrode on the cooling can already be seen by comparison to the usual cross geometry case. In the usual cross geometry, the cooling voltage was applied to the two inner junctions, and the temperature of the normal metal was measured using the two outer junctions. Back-tunnelling of quasiparticles and reabsorption of phonons contribute to the heating of the absorber [12]. With advanced geometry, the probability of these processes is decreased due to the out-diffusion of quasiparticles from the junction area. With the addition of normal metal traps, quasiparticles are allowed to dissipate their energies in the traps, thus reducing the probability of quasiparticle back-tunnelling and quasiparticle recombination in the superconductor and further enhancing the electron cooling process of the absorber.

Figure 5 shows the electron cooling curves for different temperatures for the structure with normal metal traps. In figure 5(a) we used for the experimental curves both the experimental calibration curve of the measured $V(T_{ph})$ from figure 3 and the theoretical estimation of $V(T_e)$ shown in the same figure. For figures 5(b), (c) we used only the calibration curve $V(T_e)$ giving better coincidence with theory. The best theoretical fit was obtained from equations (2), (3) using the T^6 temperature dependence of the heat flow from the phonons. The experimental results show very good agreement with theory for phonon temperatures of 300–400 mK. The leakage resistance was taken from the experiment: $R_l = 1$ MΩ. The reabsorption coefficient, $\beta = 0.02$, and the material constant, $\Sigma = 2$ nW μm^{-3} K^{-6}, were found from the fit. We speculate that the small discrepancy between theory and experiment around the optimal cooling voltage may be due to complicated interactions between the electron and phonon subsystems and the dependence on temperature.

Initially, our theoretical calculations were made using the T^5 temperature dependence of the heat flow from the phonons. Comparison with experimental results (figure 6) showed that as the voltage was increased towards the gap
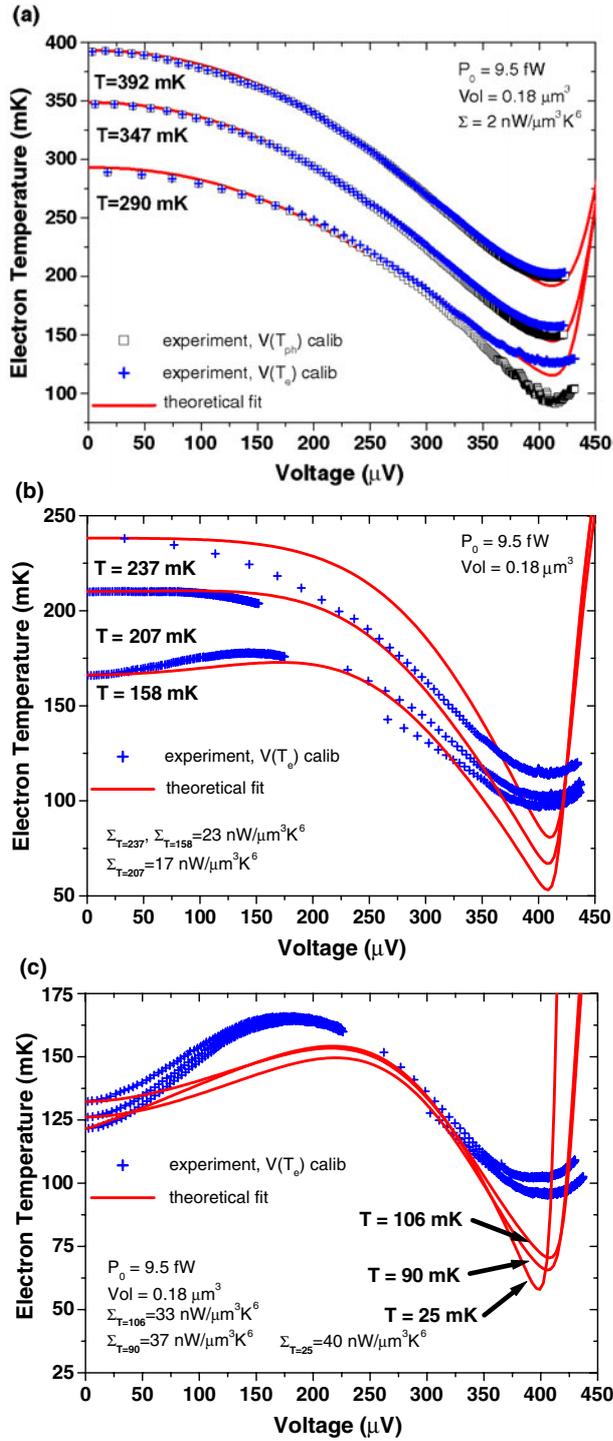
(a)

(b)

(c)

Figure 5. The main cooling curves and theoretical fit using a T^6 temperature dependence: the electron temperature as a function of the voltage across the cooling junctions for different temperature regions. The fit parameters are shown on the graphs; the leakage resistance was taken from the experiment: $R_l = 1$ MΩ, and the reabsorption coefficient, $\beta = 0.02$, was found from the fit.

voltage, electron temperature decreased faster than theory predicted. The electron cooling in experiments was even better than predicted theoretically. This suggests either a decoupling of the two phonon subsystems, i.e. the normal metal phonon and substrate phonon subsystems, or a weaker
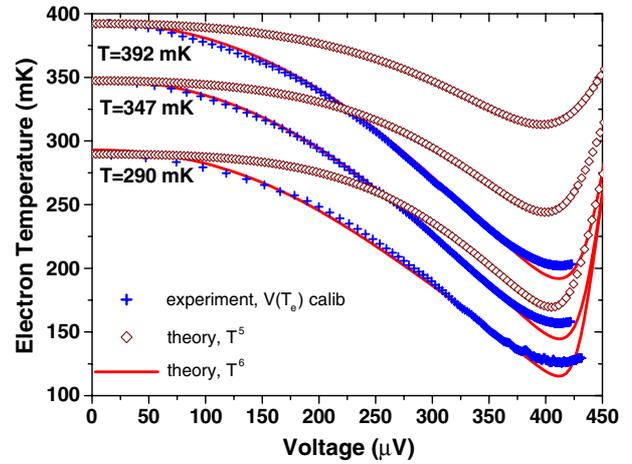

Figure 6. The main cooling curves and theoretical fit using the T^5 temperature dependence: the electron temperature as a function of the voltage across the cooling junctions for different temperature regions.

coupling between electrons and phonons in the normal metal. Thus, either an additional decoupling needs to be introduced in the theory or the calculations require a higher degree of temperature dependence. The former is not easily done as it requires the computation of a double integral. This part of our analysis is in progress.

Therefore, in our simulations, we have used a T^6 temperature dependence. The material constant, Σ, and the reabsorption coefficient, β, were used as fitting parameters. The reabsorption coefficients were approximately the same for all temperatures. On the other hand, the material constant has a dependence on temperature.

Our calculations using the sixth power for the temperature fit very nicely with our experimental data at the higher range of temperatures. At the lower range of temperatures, a heating peak (instead of a cooling one) near the zero-cooling voltage has been observed at temperatures lower than 150 mK for practically all samples. For higher cooling voltages close to the superconducting gap, the heating was converted to cooling with decreased amplitude. The leakage resistance of the tunnel junctions gives rather good fitting for this heating peak. The phonon reabsorption due to recombination of quasiparticles in superconducting electrodes gives additional improvement of the theoretical fitting but could not explain the heating peak without leakage resistance.

The problem of removing heat from the cooling junctions is the main limitation for cooler operation [13]. Making an accurate analysis of the thermal balance in the system that includes the factors that contribute to this limitation is rather complicated. However, we are aware of these factors. The efficiency of the tunnel junction as a cooler, i.e. the ratio between the total power applied to the cooler and the cooling power, is rather low and decreases with temperature. In addition, the thermal conductivity of the materials used (the substrate and Au, for example) also has a temperature dependence. In the ideal case, most of the power should be absorbed by the phonon subsystem in the superconductor and the trap. This leads to temperature gradients between the normal metal and superconductor phonon subsystems,

creating a thermal flow towards the normal metal. As the applied cooling voltage is increased towards the gap voltage, the temperature gradient also increases. As a result, the phonon temperature in the normal electrode is a function of the applied cooling voltage. All these factors contribute towards the overheating of the normal metal affecting the cooling operation at lower temperatures.

Conclusions

We have demonstrated effective electron cooling using advanced geometry of the superconducting electrodes (quadrant-shaped) and very effective Au traps near the junctions (≈ 0.5 μm) at temperatures from 25 to 500 mK. Using both improvements, we have been able to decrease the temperature of the absorber by about 200 from 300 mK. The heating peak (instead of a cooling one) near the zero-cooling voltage at temperatures lower than 150 mK observed for practically all samples has been explained by the leakage resistance of the junctions. The phonon reabsorption due to recombination of quasiparticles in superconducting electrodes gives additional improvement of the theoretical fitting but could not alone explain the heating peak. Further analysis of the data indicates decoupling between the two phonon subsystems.

References

[1] Bitterman A 1999 *Supercond. Cryoelectron.* **12** 17
[2] Leisawitz D *et al* 2000 Scientific motivation and technology requirements for the SPIRIT and SPECS far-infrared/submillimeter space interferometers *SPIE* 2000
[3] Kuzmin L 2000 *Physica* B **284–288** 2129
[4] Kuzmin L, Devyatov I and Golubev D 1998 *Proc. SPIE* **3465** 193–9
[5] Nahum M and Martinis J M 1994 *Appl. Phys. Lett.* **65** 3123
[6] Leivo M, Pecola J and Averin D 1996 *Appl. Phys. Lett.* **68** 1996
[7] Pekola J *et al* 2000 *Appl. Phys. Lett.* **76** 2782
[8] Kuzmin L 2004 *Conf. Proc. New Perspectives for Post-Herschel Far Infrared Astronomy from Space (Madrid, 1–4 Sept. 2003)* at press
[9] Golubev D and Kuzmin L 2001 *J. Appl. Phys.* **89** 6464–72
[10] Kuzmin L and Golubev D 2002 *Physica* C **372–376** 378–82
[11] Savin A *et al* 2003 *Physica* B **329–333** 1481–4
[12] Jochum J *et al* 1998 *J. Appl. Phys.* **83** 3217
[13] Savin A 2003 private communication